Making CARS better

Max Zimmerley[a], Hyun Min Kim[a], Desiré Whitmore[a], Vishnu Vardhan Krishnamachari[a], Carole Hayakawa[b], Bernard Choi[b], Vasan Venugopalan[b] and Eric O. Potma[a,b]

[a]Department of Chemistry, University of California, Irvine, Natural Sciences II, Irvine, CA 92697;
[b]Beckman Laser Institute, University of California, Irvine, 1002 Health Sciences Rd, Irvine, CA 92612

ABSTRACT

An overview is presented of recent trends in coherent anti-Stokes Raman scattering (CARS) microscopy. We briefly discuss the influence of tissue scattering on the CARS signal, methods for controlling the CARS emission and prospects for surface-enhancement of the CARS radiation.

Keywords: Coherent anti-Stokes Raman scattering, vibrational imaging, tissue scattering, interferometry

1. INTRODUCTION

CARS microscopy has morphed itself from a proof of principle technique at the turn of the last century to a widespread imaging method employed by biologists, chemists and physicists worldwide.[1-3] The broad interest for this vibrational imaging technique is not only triggered by the technologically attractive combination of high resolution imaging and coherent nonlinear spectroscopy, but also by the many new applications the technique brings to the fields of biomedical imaging and material science.

The recent recruitment of the CARS technique for studying biological samples comes in two flavors: spectroscopy and microscopy. CARS spectroscopy and micro-spectroscopy has been recognized as a swift alternative to Raman spectroscopy. Rapid detection of vibrational spectra of lipid membranes and bacterial spores are among the applications.[4, 5] CARS microscopy, on the other hand, singles out select vibrational bands for imaging purposes. CARS microscopy effectively merges Raman sensitivity with the imaging quality of a multi-photon microscope. This implies that high resolution images can be obtained with vibrational contrast and, unlike in conventional Raman microscopy, at high image acquisition speeds. These ingredients make the CARS imaging technique particularly suitable to visualize live tissues: unstained samples that require rapid imaging with chemical contrast. It is not a surprise that some of the most successful CARS microscopy applications are tissue imaging studies, ranging from resolving fat deposits in skin to myelin imaging in spinal cords.[6-8]

By moving into the biomedical imaging field, CARS microscopists are facing several challenges. One of these challenges is to make the CARS technique a reliable reporter of molecular concentration. The complex coherent signal formation, along with tissue scattering effects, limits an accurate quantitative assessment of CARS tissue images. The ubiquitous nonresonant background complicates analysis as well. To make CARS more quantitative, the effects of signal generation and tissue scattering need to be disentangled. Next, better control of the CARS generation process is desired to optimize the molecular informational content of the signal.

In this overview we present several strategies for understanding and improving CARS imaging in tissues. The issue of scattering is approached both experimentally and theoretically, and conclusions are drawn on the quantitative reporting capabilities of the CARS microscopy technique. We also introduce several ways to control the CARS emission for improving signal contrast. Finally, prospects for higher spatial resolution and single molecule detection are discussed.

2. DYNAMIC TISSUE IMAGING WITH CARS

One of the major advantages of CARS microscopy over Raman microscopy is its imaging speed. While out of reach on a regular Raman microscope, acquisition rates of more than one frame per second are the norm in CARS microscopy. Consequently, CARS is the method of choice for visualizing rapid changes in tissues. In particular, CARS enables real-

time mapping of the diffusion of applied chemicals through tissue. Such diffusion processes are relevant to the study of transport of topically applied drugs through the skin.

We have studied the diffusion of glycerol, a major component of skin health care products, and dimethyl-sulfoxide (DMSO) through human skin. Both chemicals, when topically applied, induce a temporary transparency of the skin when applied topically. Skin transparency significantly facilitates optical investigations at greater depths into the tissue, and aids visualization of tissue structures typically blurred by the opacity of dermal and epidermal layers.[9] Nonetheless, the biophysical origin of the optical clearing phenomenon is currently under debate. One of the difficulties in unraveling the mechanism of optical skin clearing is that the local, time-varying concentration of skin-clearing agent is typically inaccessible in conjunction with the changing tissue scattering coefficient. With its rapid imaging capability and chemical selectivity, CARS microscopy is the ideal method to tackle this problem. Vice versa, the changing refractive properties of the tissue over time provide a systematic way for investigating the effect of scattering on the CARS signal.

Figure 1 shows the temporal dependence of the CARS signal of DMSO applied to a ~1 mm thick slab of excised human skin. DMSO is conveniently addressed through its 2913 cm^{-1} symmetric CH_3 stretching vibration. The signal is collected in the forward- and epi-direction simultaneously, along with the transmittance of the incident light through the tissue slab. As expected, the tissue transmittance increases over time. In addition, several interesting features are observed. First, during the first few minutes, the transmittance increases much faster than the forward CARS (F-CARS) signal. This indicates that the changing scattering properties of the tissue do not linearly scale with the DMSO concentration. Second, while the F-CARS signal rises at all times, the epi-CARS signal (E-CARS) first dips and rises only after ~10 minutes. This effect is explained by the fact that the majority of E-CARS signal results from back-scattering of forward propagating CARS radiation. Increased transmission implies reduced scattering and hence less E-CARS signal. The higher DMSO concentrations are reflected in the E-CARS channel only after the initial loss in scattering is balanced out by the stronger forward propagating CARS levels. By comparing the F-CARS and E-CARS signal with the transmission changes, quantitative conclusions can be drawn on how the DMSO concentration affects the tissue transparency.
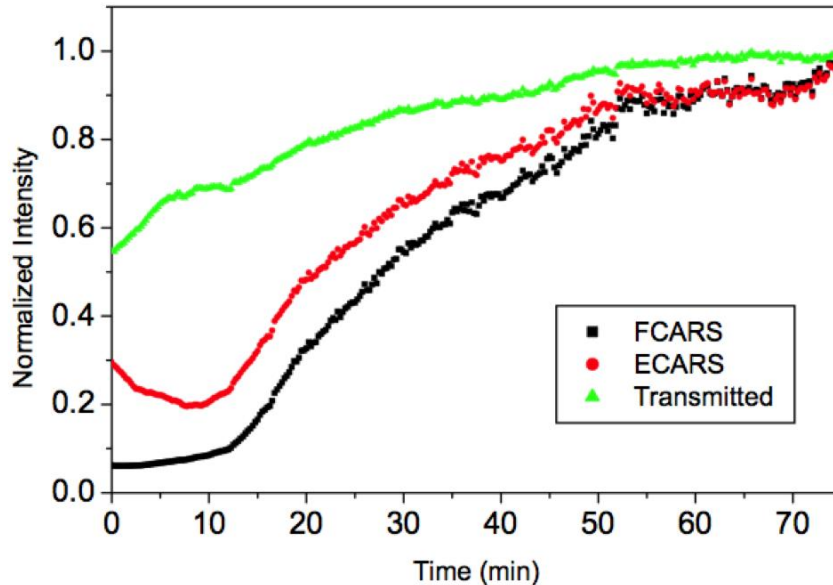
Figure 1. Dynamic measurement of DMSO applied to human skin. The total integrated CARS signal from DMSO is plotted as a function of time after application. The tissue scattering is reduced due to the effect of the DMSO. Note the difference in the forward and backward CARS signals, indicative of the different role scattering plays in each of the these detection channels.

The main lessons from these studies are twofold: 1) CARS is an excellent method for resolving the time-varying changes of applied chemical compounds to the tissue; 2) Tissue scattering profoundly affects the detected CARS signal. It was also seen that the forward CARS signal and epi-directed CARS signal are affected differently. Direct information on the scattering of the tissue can be obtained by relating the F-CARS to the E-CARS signal. While the current studies benefit from detecting both the forward and epi-signals simultaneously, in typical imaging studies the forward channel is not available due to opaqueness of the sample. A quantitative interpretation of the CARS signal requires, therefore, a closer look at the influence of tissue scattering onto the detected signal.
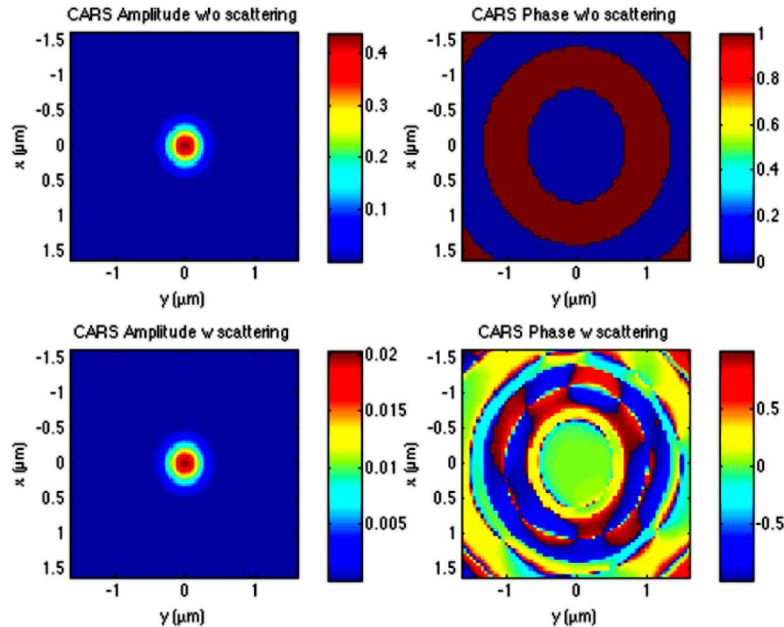
3. INFLUENCE OF TISSUE SCATTERING

Previous studies on the influence of tissue scattering on the image quality in multiphoton microscopy have revealed that nonlinear signals are considerably affected by the depleted number of photons at the focal volume.[10] In nonlinear coherent microscopy, however, it is expected that the signal is not only affected by the loss of incident field amplitude but also by the distortion of the phase of the fields. The problem of tissue scattering in nonlinear coherent microscopy can be divided into three parts: 1) Pre-generation: scattering and subsequent distortion of the amplitude and phase of the incident fields; 2) Generation: affected coherent signal generation due to distorted incident fields; 3) Post-generation: scattering and subsequent distortion of the propagating signal.

We have started Monte Carlo studies to examine in detail the influence of scattering at the pre-signal generation and signal generation level. It is a challenge to incorporate phase effects into Monte Carlo simulations, which are usually based on the particle approximation for the photon. To gain insight in the phase distortion, typically considered a field effect, we have taken the following approach. The incident field $A(x,y)$ at the focal plane is modeled as:

$$A(x,y) = G(x,y) \otimes E(x,y) \tag{1}$$

where $G(x,y)$ is a propagator that includes the distortion of the complex field, and $E(x,y)$ is the undistorted field distribution in the focal plane.

Figure 2. Influence of tissue scattering on the CARS excitation field. The CARS excitation filed is defined by $E_p^2 E_S^*$, where E_p is the pump filed and E_S the Stokes field. Monte Carlo calculations were performed with 10^7 photons. The microscope objective was a 1.1 NA water immersion lens.

In the absence of scattering, the propagator is determined by the pathways of photons launched from the aperture of the objective lens and converging into a single point at the focal plane. Eq (1) then predicts that the focal field is simply the diffraction limited focal field $E(x,y)$. In the presence of scattering, the photons no longer converge to a single point. In addition, the arrival times (or phase) of individual photons in the focal plane will no longer be single-valued. From the collected photons at the focal plane, we determine the overall phase and amplitude distribution, from which the complex function $G(x,y)$ is calculated.

Figure 2 shows the calculated amplitude and phase of the CARS excitation field with and without scattering. The sample was considered to be a 100 μm thick 10% intralipid solution with well-defined scattering, absorption and anisotropy parameters. Several features can be observed: 1) While the overall amplitude decreases, the normalized field distribution is barely affected by the scattering process; 2) Qualitatively, the phase distribution is significantly affected by tissue scattering. Nonetheless, at the location of highest field amplitudes the phase profile is virtually flat. While, the overall phase distortions may be considerable, their influence on the CARS signal are surprisingly small. Our calculations indicate tissue scattering affects the CARS signal predominantly through a loss of amplitude of the incident fields, and only secondarily through loss of phase purity.

4. CONTROLLING CARS

4.1 Spatial-phase control: Focus-engineered CARS (FE-CARS)

In CARS, molecular oscillators are set in motion throughout the focal volume with a well-defined phase. This implies that there is a phase relationship among all the oscillators. In the focal plane, for instance, all the oscillators will be driven with the same phase with conventional CARS excitation. The CARS waves that are subsequently emitted from the focal plane will be constructively interfering along the propagation axis. When using typical Gaussian beams in CARS microscopy, strong signals are observed in the forward propagating direction due to constructive interference, whereas much weaker signals are seen in the backward direction because of destructive interference of the emitted waves.

The CARS emission can be changed when the oscillators are driven with different phases at different locations in the focal volume. Such can be accomplished by phase shaping of the incident focal fields. The result of focus-engineering is that the emitted waves can be made to interfere in a different fashion then seen in regular CARS. By controlling the phase distribution in the focal spot, the CARS emission can be controlled and contrast in the microscope can be improved accordingly.

One example of a transverse phase-profile that leads to new contrast in the CARS microscope is a lateral π phase step, reminiscent of the phase step in a Hermite Gaussian 01 beam (HG01). When the Stokes beam is dressed with such a phase step, a CARS excitation field results (see Figure 3) in which one half of the focal volume will be driven out-of-phase relative to the other half. Consequently, destructive interference along the propagation axis is observed, thereby effectively switching off the CARS signal. Interestingly, it has been shown that the spatial phase step can be compensated by the spectral phase step in the vicinity of vibrational resonances.[11, 12] This results in strong signals from vibrationally resonant interfaces, effectively accentuating resonant objects in the image. Such differential contrast may have interesting applications in imaging of cellular samples or thin film materials. In addition, under conditions of limited scattering-induced phase distortions, the focus-engineering technique may also prove useful for object highlighting in tissue samples.
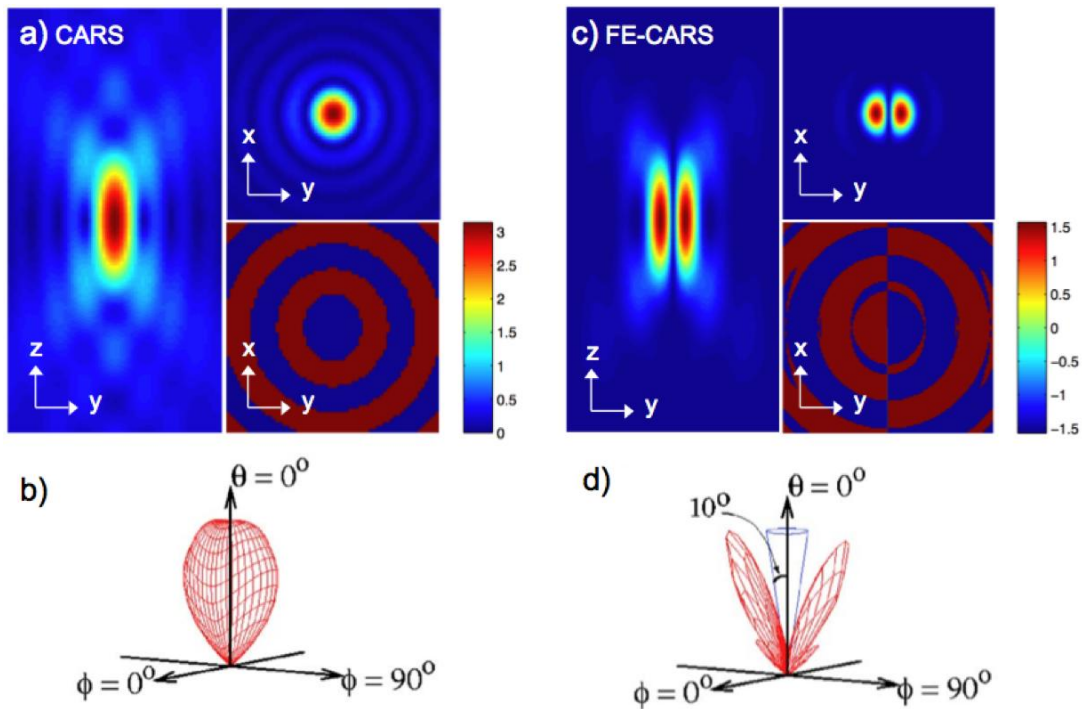
Figure 3. Principle of FE-CARS. In a) the normal CARS excitation field is shown for a NA 1.1 water immersion lens, for the xy and yz planes. The phase of the excitation field is also given, showing discrete π-phase steps of radial symmetry. This excitation field gives rise CARS emission directed along the optical axis, depicted in b). In c) the FE-CARS excitation field is shown for the case of a HG01 phase pattern. The dark part of the focus corresponds to the presence of a π-phase step in the y-direction. The CARS emission is no longer directed along the optical axis, as shown in d), because of the destructive interference along the optical axis induced by the engineered phase step. All yz images are 3 x 6 μm, while xy images are 3 x 3 μm. Excitation and emission fields are calculated according to the method described in Ref. [11]

4.2 Emission control: CARS interferometry

Phase shaping of the incident beams is one avenue towards controlling the overall CARS emission process. Another way to exert control over the CARS signal is achieved by interfering the CARS field with an external field at the anti-Stokes frequency. It has been shown that the CARS interferometry approach allows efficient suppression of the nonresonant background signal and exclusive detection of the imaginary part of the nonlinear susceptibility.[13] An interesting form of control is realized when the external field is co-propagating with the incident pump and Stokes fields. In this case, interference takes place directly in the sample at the location of the focal volume. When the external field is in phase with the CARS polarization, a strong signal is detected, while the signal is depleted when the external phase and the CARS polarization are out-of-phase. In the latter case, the amplitudes of the fields can be chosen such that no signal at the anti-Stokes frequency is detected, effectively switching off the all the signal at the anti-Stokes frequency. Note that not only the CARS emission is suppressed, but that also the external field is depleted in the process.

Switching off the anti-Stokes radiation raises the question of energy conservation. It is interesting to note that the depletion of radiation in the forward detection direction is not compensated by an increased emission in the backward direction, as can be seen in Figure 4. In that sense, the sample plays a role very different from the role of a beam splitter in a regular interferometer experiment. Unlike a beam splitter, the sample mediates the flow of energy into multiple channels as constituted by the pump, Stokes, anti-Stokes and emission fields. By blocking the anti-Stokes radiation channel, energy flows into different channels as determined by the phase relationship among the fields.
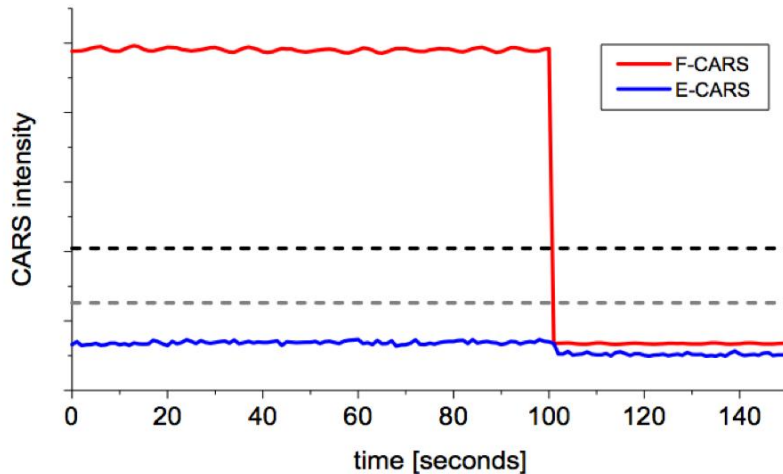
Figure 4. Switching off of the CARS radiation with an external field. The anti-Stokes external field is initially in-phase with the CARS signal, resulting in an amplified signal. At the 100 s time point, the external field is switched out-of-phase with the CARS signal. The detected signal at the anti-Stokes frequency is almost completely depleted. Note that the loss in the forward detection direction is not compensated by an increase in the epi-direction. The average intensity of the CARS signal without the external field is indicated by the black dashed line, whereas the intensity of the external beam is indicated by the gray dashed line. Note also that the depleted signal level is lower than the intensity of the incoming external beam.

The ability to completely switch off the anti-Stokes radiation with an external field opens up possibilities to develop phase-only analogs of stimulated emission depletion (STED) microscopy.[14] Depletion of CARS emission in select portions of the focal volume can be achieved by combining focus-engineering with an external depletion field. Studies in this area are currently underway.

5. STRONGER CARS

Can CARS be used to detect single molecules? Single molecule CARS studies would not only open possibilities for rapid molecular sensing but also introduce a new field of optical investigation directed at the coherent properties of single molecules. Unfortunately, under regular off-resonance conditions, the CARS response from a single (local mode) oscillator is below the detection limit. Notable exceptions exist for molecules with strongly delocalized modes such as the D and G bands of carbon nanotubes, which exhibit Raman cross sections many orders of magnitude higher relative to a typical local mode. Carbon nanotubes have previously been imaged with Raman microscopy.[15] Figure 5 shows a CARS image of a folded single nanotube tethered to a Titanium electrode. Incident pulse energies were as low as 10 pJ, underlining the strong response from the nanotubes.
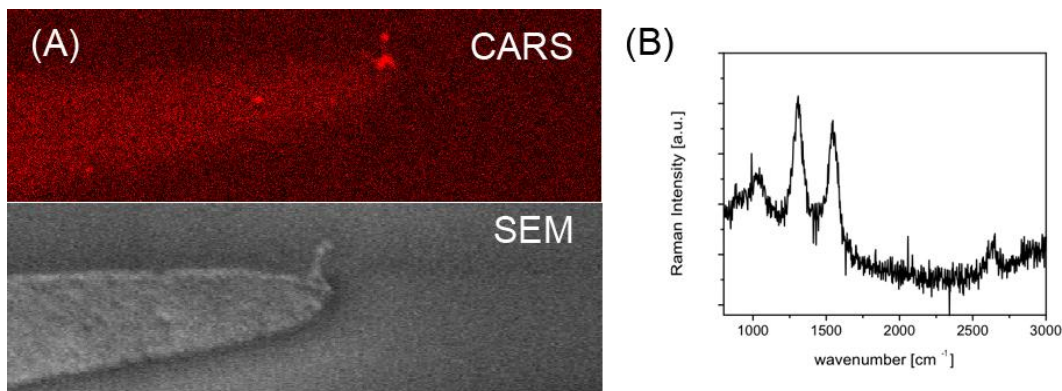

Figure 5. (A) CARS image at 1315 cm^{-1} of single carbon nanotubes, attached to a Titanium electrode. The SEM image, taken at the same location, confirms that this is a single folded carbon nanotube. The corresponding Raman spectrum of the carbon nanotube is shown in (B).

To detect molecules with much smaller Raman cross sections through CARS, enhancement methods are inevitable. Inspired by the principle of surface enhanced Raman scattering (SERS), recent studies have indicated that the CARS signal may benefit from the surface enhanced fields at metallic interfaces.[16, 17] We have found that many traditional SERS nanostructures, such as silver and gold colloids, are not suitable for SE-CARS. We have determined that most SERS substrates a) exhibit a strong and broad non-vibrational emission under ultrafast excitation; b) show photodamage under benign (a few mW) excitation conditions; c) have ill-defined surface plasmon fields, in terms of location and orientation.

A well-defined plasmonic substrate is key to reliable and reproducible SE-CARS experiments. We have chosen to work with gold nanowires (30 – 500 nm wide, hundreds of μm long) because of their a) easily tunable plasmon frequencies; b) well-defined location and orientation of the plasmon-enhanced fields; c) robustness; d) easy of manipulation with electrodes.

We have measured the plamon-enhanced CARS response from gold nanowires with various plasmon frequencies. The CARS emission displays a very distinct polarization dependence, shown in Figure 6, which indicates that there is a well-defined mode that is resonantly addressed by the incident pulses. We found that at the CARS emission wavelength, the signal is devoid of other nonlinear emission (fluorescence, white light generation) processes that are commonly observed under ultrafast excitation of metallic structures. The ability to accurately drive the plasmon mode will be imperative for successful and reliable single molecule experiments.
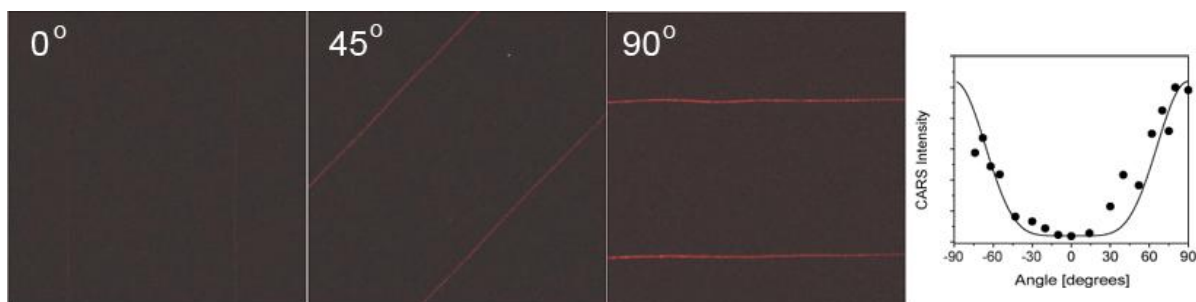
Figure 6. Orientation dependence of the purely plasmon-enhanced CARS emission from single 400-nm wide gold nanowires. Two wires are imaged as a function of longitudinal angle θ relative to the polarization of the beams, The CARS signal follows an $cos^6\theta$ dependence. Similar results are obtained for 100-nm and 60-nm wide wires.

REFERENCES

1. J. X. Cheng and X. S. Xie, "Coherent anti-Stokes Raman scattering microscopy: instrumentation, theory and applications," J. Phys. Chem. B **108**, 827-840 (2004).
2. J. X. Cheng, "Coherent anti-Stokes Raman scattering microscopy," Appl. Spectrosc. **91**, 197-208 (2007).
3. A. Volkmer, "Vibrational imaging and microspectroscopies based in coherent anti-Stokes Raman scattering microscopy," J. Phys. D **38**, R59-R81 (2005).
4. G. W. Wurpel, J. M. Schins, and M. Muller, "Direct measurement of chain order in single phospholipid mono- and bilayers with multiplex-CARS," J. Phys. Chem. B **108**, 3400-3403 (2004).
5. G. I. Petrov, R. Arora, V. V. Yakolev, X. Wang, A. V. Sokolov, and M. O. Scully, "Comparison of coherent and spontaneous Raman microspectroscopies for noninvasive detection of single bacterial endospores," Proc. Natl. Acad. Sci. USA **104**, 7776-7779 (2007).
6. C. L. Evans, E. O. Potma, M. Puoris'haag, D. Cote, C. Lin, and X. S. Xie, "Chemical imaging of tissue *in vivo* with video-rate coherent anti-Stokes Raman scattering (CARS) microscopy," Proc. Natl. Acad. Sci. USA **102**, 16807-16812 (2005).
7. T. B. Huff and J. X. Cheng, "In vivo coherent anti-Stokes Raman scattering imaging of sciatic nerve tissues," J. Microsc. **225**, 175-182 (2007).
8. H. Wang, Y. Fu, P. Zickmund, R. Shi, and J. X. Cheng, "Coherent anti-Stokes Raman scattering imaging of live spinal tissues," Biophys. J. **89**, 581-591 (2005).
9. V. V. Tuchin, "Optical clearing of tissues and blood using the immersion method," J. Phys. D **38**, 2497-2518 (2005).
10. A. K. Dunn, V. P. Wallace, M. Coleno, M. W. Berns, and B. J. Tromberg, "Influence of optical properties on two-photon fluorescence imaging in turbid samples," Appl. Opt. **39**, 1194-1201 (2000).

11. V. V. Krishnamachari and E. O. Potma, "Focus-engineered coherent anti-Stokes Raman scattering: a numerical investigation," J. Opt. Soc. Am. A **24**, 1138-1147 (2007).
12. V. V. Krishnamachari and E. O. Potma, "Detecting lateral interfaces with focus-engineered coherent anti-Stokes Raman scattering microscopy," J. Raman Spectrosc., in press. (2007).
13. E. O. Potma, C. L. Evans, and X. S. Xie, "Heterodyne coherent anti-Stokes Raman scattering (CARS) imaging," Opt. Lett. **31**, 241-243 (2006).
14. T. A. Klar, S. Jakobs, M. Dyba, A. Egner, and S. W. Hell, "Fluorescence microscopy with diffraction resolution barrier broken by stimulated emission," Proc. Natl. Acad. Sci. USA **97**, 8206-8210 (2000).
15. A. Hartschuh, H. N. Pedrosa, L. Novotny, and T. D. Krauss, "Simultaneous fluorescence and Raman scattering from single carbon nanotubes," Science **301**, 1354-1356 (2003).
16. T. Ichimura, N. Hayazawa, M. Hashimoto, Y. Inouye, and S. Kawata, "Tip-enhanced coherent anti-Stokes Raman scattering for vibrational nanoimaging," Phys. Rev. Lett. **92**, 220801 (2004).
17. T. W. Koo, S. Chan, and A. A. Berlin, "Single-molecule detection of biomolecules by surface-enhanced coherent Raman scattering," Opt. Lett. **30**, 1024 (2005).